



## Time domain analysis of a viscoelastic rotor using internal variable models

Michael I. Friswell<sup>\*,a</sup>, Jayanta K. Dutt<sup>b</sup>, Sondipon Adhikari<sup>a</sup>, Arthur W. Lees<sup>a</sup>

<sup>a</sup> School of Engineering, Swansea University, Singleton Park, Swansea SA2 8PP, UK

<sup>b</sup> Department of Mechanical Engineering, Indian Institute of Technology, Delhi, Post Office Hauz Khas, New Delhi 110016, India

### ARTICLE INFO

#### Article history:

Received 24 September 2009

Received in revised form

4 June 2010

Accepted 8 June 2010

Available online 16 June 2010

#### Keywords:

Viscoelastic

ADF

ATF

### ABSTRACT

Damping in the stator of a rotating machine is able to reduce the unbalance response, and increase the speed where the stability limit is reached. However, damping in the rotor is destabilising and the analysis of rotors with internal viscous damping is well established. The drive towards composite and laminated rotors mean that the viscous damping model is not always appropriate, and viscoelastic material models whose properties depend on frequency should be used. These properties may be measured experimentally and the analysis of structures containing viscoelastic material materials may be performed in the time domain using the ADF, ATF or GHM methods. This paper extends this analysis to rotors containing viscoelastic materials using the ATF approach. Other internal variable formulations for viscoelastic material may be used following the approach adopted in this paper with only slight modifications. Viscous damping in the rotor produces a skew-symmetric component in the 'stiffness' matrix; for viscoelastic models the skew-symmetric term appears in the internal variable equations. This paper gives an example to demonstrate the calculation of the stability limit speed for a machine.

© 2010 Elsevier Ltd. All rights reserved.

### 1. Introduction

The stability, steady state unbalance and the transient responses of a machine depend on the stiffness and damping characteristics of the complete machine. Support damping is able to improve the stability and transient behaviour, and elastomer supports are a cheap and convenient way of achieving this. The optimum parameters for such supports have been considered [1–4]. Bormann and Gasch [4] also included a frequency dependent elastomer modulus in their analysis. However the use of elastomers makes the analysis much more difficult, particularly where time dependence is important. For example, the effects of temperature and material ageing make the standard methods of machine balancing ineffective, since either the influence coefficients or the modes change with time. The analysis of non-linear machines, for example those with cracks in the shaft, is often best undertaken using a time domain method. The response of a machine during a run-up or run-down is a transient response that should be simulated in the time domain. Friswell et al. [5] included the effects of temperature of the viscoelastic material into the analysis, together with a simple

energy dissipation model, to demonstrate the effects on the steady state response and balancing. This paper considers the analysis of a viscoelastic rotor and concentrates on the prediction of the stability limit speed for a machine. Roy et al. [6] considered this problem by integrating the stress directly. Genta [7] accounted for internal damping in the rotor using a Voigt–Boit model. This paper takes a different approach by transforming the physical and internal variables to account for the rotor spin.

The damping model used is generalized from viscous to non-viscous. Adhikari and Woodhouse [8,9] presented a systematic study on the analysis and identification of damped mechanical systems, focused on non-viscously damped MDOF linear vibrating systems. Woodhouse [10] obtained approximate expressions for damped natural frequencies, complex modes and transfer functions for linear systems with light viscous and non-viscous damping. Bagley and Torvik [11,12] presented a finite element formulation and closed form solutions in the Laplace domain for the dynamics of damped bar and beam structures. They showed that the fractional derivative model has some attractive features, and that very few empirical parameters are required to model the viscoelastic material over a wide frequency range.

An alternative approach to modelling the dynamics of elastomers is to introduce additional co-ordinates to account for the frequency dependent and hysteretic behaviour. Motivated by the need to produce finite element models (FEMs) that are capable of predicting the dynamic response of a structure or component, Hughes and his co-workers [13,14] and Lesieutre and his co-workers [15–18] developed independent means of

\* Corresponding author.

E-mail addresses: [m.i.friswell@swansea.ac.uk](mailto:m.i.friswell@swansea.ac.uk) (M.I. Friswell), [jkdudd@mech.iitd.ernet.in](mailto:jkdudd@mech.iitd.ernet.in) (J.K. Dutt), [s.adhikari@swansea.ac.uk](mailto:s.adhikari@swansea.ac.uk) (S. Adhikari), [a.w.lees@swansea.ac.uk](mailto:a.w.lees@swansea.ac.uk) (A.W. Lees).

URLS: <http://michael.friswell.com> (M.I. Friswell), <http://engweb.swan.ac.uk/~adhikaris> (S. Adhikari).

## Nomenclature

<b>B</b>	coupling matrix in the equations of motion for the physical degrees of freedom vector	<b>K</b>	global physical stiffness matrix
<b>B<sub>i</sub></b>	coupling matrix in the equations of motion for the physical degrees of freedom, relating to the <i>i</i> th internal variable vector	<b>K<sub>e</sub></b>	stiffness matrix for element <i>e</i>
<b>C</b>	matrix coefficient for the first order derivative in the equations of motion for the internal variables	<b>M</b>	global physical mass matrix
<b>C<sub>i</sub></b>	matrix coefficient for the first order derivative in the equation of motion for internal degrees of freedom vector <i>i</i>	<b>p</b>	vector of internal degrees of freedom
<b>D</b>	speed dependent matrix coefficient for the zeroth order derivative in the equations of motion for the internal variables	<b>p<sub>ei</sub></b>	<i>i</i> th internal variable vector for element <i>e</i>
<b>D<sub>i</sub></b>	speed dependent matrix coefficient for the zeroth order term in the stationary frame for internal variable vector <i>i</i> , defined by Eq. (20)	<b>q</b>	vector of physical degrees of freedom
<b>F</b>	coupling matrix in the equations of motion for the internal degrees of freedom vector	<b>Q<sub>e</sub></b>	elastic and viscoelastic force for element <i>e</i>
<b>f</b>	external force vector in physical degrees of freedom	<b>q<sub>e</sub></b>	nodal displacement vector for element <i>e</i>
<b>F<sub>i</sub></b>	coupling matrix in the equations of motion for internal degrees of freedom vector <i>i</i>	<b>T<sub>2n(t)</sub></b>	transformation from rotating to stationary coordinates for <i>n</i> pairs of degrees of freedom
<b>G</b>	global physical gyroscopic matrix	<b>E</b>	Young's modulus
<b>H</b>	speed independent matrix coefficient for the zeroth order derivative in the equations of motion for the internal variables	<b>G(s)</b>	frequency dependent material modulus, given by Eq. (12)
<b>H<sub>i</sub></b>	matrix coefficient for the zeroth order derivative in the equation of motion for internal degrees of freedom vector <i>i</i>	<b>l<sub>e</sub></b>	second moment of area for element <i>e</i>
		<b>m</b>	number of internal variables in the viscoelastic model for each physical coordinate
		<b>ℓ<sub>e</sub></b>	length of element <i>e</i>
		<b>α<sub>i</sub>, δ<sub>i</sub>, b<sub>i</sub></b>	ATF viscoelastic model parameters for the <i>i</i> th internal variable
		<b>γ<sub>i</sub></b>	parameter derived from $\gamma_i \alpha_i E = \delta_i^2 b_i$
		<b>φ(t)</b>	angle of rotation of the rotor
		<b>K̂<sub>e</sub></b>	element stiffness matrix with $E=1$
		<b>~</b>	tilde denotes a variable in the rotating frame of reference
		<b>ADF</b>	anelastic displacement fields
		<b>ATF</b>	augmenting thermodynamic fields
		<b>FEM</b>	finite element method
		<b>GHM</b>	Golla–Hughes–McTavish
		<b>MSE</b>	modal strain energy

augmenting an FEM with new coordinates containing damping properties found from material loss factor curves. The GHM method [13,14] uses a second order physical co-ordinate system and the Lesieutre approaches [15–18] use first order state space methods called the anelastic displacement fields (ADF) or the augmenting thermodynamic fields (ATF) methods. Both are superior to the modal strain energy (MSE) method proposed by Rogers et al. [19]. While the MSE method is substantially easier to use, both the ADF and the GHM methods are more accurate. These two more complex approaches are able to account for damping effects over a range of frequencies, complex mode behaviour, transient responses and both time and frequency domain modelling. Inman [20] applied the GHM approach to simple beams and Banks and Inman [21] provided an alternate time domain method for modelling hysteresis. Friswell et al. [22] considered the curve fitting required in the GHM approach.

The modelling of the elastomer often uses internal variables to model the frequency dependence of the modulus. The approach starts with data for the experimentally obtained complex modulus or loss factor as a function of frequency. These data are available from manufacturers of viscoelastic material and are curve fitted by a rational polynomial. This rational polynomial, with coefficients reflecting the material properties of the test specimen, is next used to represent the Laplace Transform of the hysteretic stress–strain relationship. The result is combined with the undamped model of the structure to produce a final model containing expanded co-ordinates and a damping matrix that captures the transient decay and complex mode behaviour of the machine with the viscoelastic components. The approach adopted here is the ATF approach incorporating temperature dependence [23–25]. Of course other internal variable formulations for viscoelastic material (for example ADF or GHM) may be used

following the approach adopted in this paper with only slight modifications.

## 2. Element matrices in the rotating frame

The element mass and stiffness matrices for the shaft are identical to the standard formulation. Lesieutre and Mingori [15] gave the finite elements for Euler–Bernoulli beam bending. These expressions are extended to the shaft model by considering the two transverse directions independently.

The element matrices in rotating coordinates are based on the physical nodal displacement vector given by [26]

$$\tilde{\mathbf{q}}_e = [\tilde{u}_1 \quad \tilde{v}_1 \quad \tilde{\theta}_1 \quad \tilde{\psi}_1 \quad \tilde{u}_2 \quad \tilde{v}_2 \quad \tilde{\theta}_2 \quad \tilde{\psi}_2]^T \quad (1)$$

where *u* and *v* are nodal displacements in the *x* and *y* directions, *θ* and *ψ* are rotations about the *x* and *y* axes, the subscripts 1 and 2 denote the two ends of the shaft element, and the tilde denotes that the variables are defined in the rotating frame of reference. The *i*th internal variable vector, defined in the rotating frame, is

$$\tilde{\mathbf{p}}_{ei} = [\tilde{p}_{u1i} \quad \tilde{p}_{v1i} \quad \tilde{p}_{u2i} \quad \tilde{p}_{v2i}]^T \quad (2)$$

where the subscripts *u* and *v* denote the two directions for the beam model. Fig. 1 shows the shaft element and the associated degrees of freedom. The standard cubic shape functions are used to interpolate the physical deformation within the element, and linear shape functions are used to interpolate the internal variables. Note that  $i=1, \dots, m$ , since there are *m* internal variables, arising from the *m* first order terms in the frequency dependent viscoelastic material modulus.

Here we are concerned with the elastic forces arising from the shaft element and the viscoelastic material properties. Following

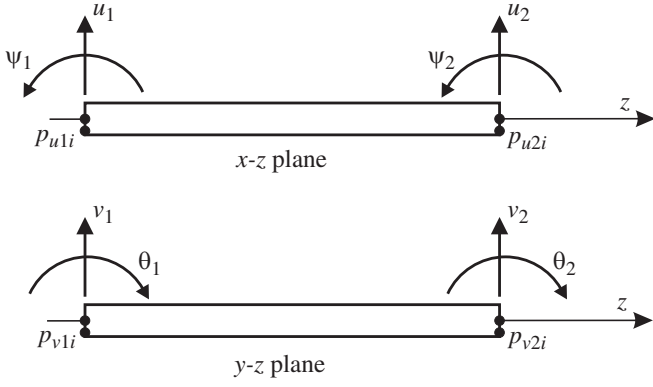


Fig. 1. The definition of the degrees of freedom for the shaft element.

the development for the ATF method for static structures [15], the force is

$$\tilde{\mathbf{Q}}_e = -\mathbf{K}_e \tilde{\mathbf{q}}_e + \sum_{i=1}^m \mathbf{B}_i \tilde{\mathbf{p}}_{ei} \quad (3)$$

where

$$\mathbf{C}_i \dot{\tilde{\mathbf{p}}}_{ei} + \mathbf{H}_i \tilde{\mathbf{p}}_{ei} = \mathbf{F}_i \tilde{\mathbf{q}}_e \quad \text{for } i = 1, \dots, m. \quad (4)$$

The stiffness matrix is standard [26] and for Euler–Bernoulli beam theory is

$$\mathbf{K}_e = \frac{EI_e}{\ell_e^3} \begin{bmatrix} 12 & 0 & 0 & 6\ell_e & -12 & 0 & 0 & 6\ell_e \\ 0 & 12 & -6\ell_e & 0 & 0 & -12 & -6\ell_e & 0 \\ 0 & -6\ell_e & 4\ell_e^2 & 0 & 0 & 6\ell_e & 2\ell_e^2 & 0 \\ 6\ell_e & 0 & 0 & 4\ell_e^2 & -6\ell_e & 0 & 0 & 2\ell_e^2 \\ -12 & 0 & 0 & -6\ell_e & 12 & 0 & 0 & -6\ell_e \\ 0 & -12 & 6\ell_e & 0 & 0 & 12 & 6\ell_e & 0 \\ 0 & -6\ell_e & 2\ell_e^2 & 0 & 0 & 6\ell_e & 4\ell_e^2 & 0 \\ 6\ell_e & 0 & 0 & 2\ell_e^2 & -6\ell_e & 0 & 0 & 4\ell_e^2 \end{bmatrix}. \quad (5)$$

The other matrices are [15]

$$\mathbf{C}_i = \frac{\ell_e}{6} \begin{bmatrix} 2 & 0 & 1 & 0 \\ 0 & 2 & 0 & 1 \\ 1 & 0 & 2 & 0 \\ 0 & 1 & 0 & 2 \end{bmatrix}, \quad \mathbf{H}_i = b_i \mathbf{C}_i \quad (6)$$

and

$$\mathbf{B}_i = \frac{\delta_i \ell_e}{\ell_e} \begin{bmatrix} -1 & 0 & 1 & 0 \\ 0 & -1 & 0 & 1 \\ 0 & \ell_e & 0 & 0 \\ -\ell_e & 0 & 0 & 0 \\ 1 & 0 & -1 & 0 \\ 0 & 1 & 0 & -1 \\ 0 & 0 & 0 & -\ell_e \\ 0 & 0 & \ell_e & 0 \end{bmatrix}, \quad \mathbf{F}_i = \frac{b_i}{\alpha_i \ell_e} \mathbf{B}_i^T. \quad (7)$$

Note that  $\mathbf{C}_i$  and  $\mathbf{H}_i$  are symmetric and positive definite.

The corresponding frequency dependent material model may be recovered by substituting for  $\tilde{\mathbf{p}}_{ei}$  in the physical equations of motion in the Laplace domain. Thus, from Eqs. (3) and (4), the nodal force is

$$\tilde{\mathbf{Q}}_e = -\mathbf{K}_e \tilde{\mathbf{q}}_e + \sum_{i=1}^m \mathbf{B}_i \tilde{\mathbf{p}}_{ei} = -\mathbf{K}_e \tilde{\mathbf{q}}_e + \sum_{i=1}^m \mathbf{B}_i [\mathbf{C}_i s + \mathbf{H}_i]^{-1} \mathbf{F}_i \tilde{\mathbf{q}}_e. \quad (8)$$

Using Eq. (6) this becomes

$$\tilde{\mathbf{Q}}_e = -\mathbf{K}_e \tilde{\mathbf{q}}_e + \sum_{i=1}^m \frac{1}{s+b_i} \mathbf{B}_i \mathbf{C}_i^{-1} \mathbf{F}_i \tilde{\mathbf{q}}_e. \quad (9)$$

Finally,  $\mathbf{B}_i$ ,  $\mathbf{C}_i$  and  $\mathbf{F}_i$  have been chosen such that  $\mathbf{B}_i \mathbf{C}_i^{-1} \mathbf{F}_i = \gamma_i \mathbf{K}_e$ , where the scalar constant is given by  $\gamma_i \alpha_i E = \delta_i^2 b_i$ . Thus

$$\tilde{\mathbf{Q}}_e = - \left[ E - \sum_{i=1}^m \frac{\delta_i^2 b_i}{\alpha_i s + b_i} \right] \hat{\mathbf{K}}_e \tilde{\mathbf{q}}_e \quad (10)$$

where  $\hat{\mathbf{K}}_e$  is the element stiffness matrix with unit Young’s modulus ( $E=1$ ).

This is equivalent to

$$\tilde{\mathbf{Q}}_e(s) = -G(s) \hat{\mathbf{K}}_e \tilde{\mathbf{q}}_e \quad (11)$$

where  $G(s)$  is the frequency dependent material modulus given by

$$G(s) = E - \sum_{i=1}^m \frac{\delta_i^2 b_i}{\alpha_i s + b_i}. \quad (12)$$

Other decompositions of the stiffness matrix are possible, leading to different internal variables and hence different definitions of the matrices, but leading to the same equivalent material properties. However, the definition above has the advantage that the internal variables are defined at the nodes and hence lead to a continuous ATF variable across elements. This allows for the easy assembly of the finite element matrices.

### 3. Transforming the element matrices to the stationary frame

We include rotation via a transformation matrix  $\mathbf{T}_2(t)$  for each pair of degrees of freedom defined as

$$\mathbf{T}_2 = \begin{bmatrix} \cos \phi & -\sin \phi \\ \sin \phi & \cos \phi \end{bmatrix} \quad (13)$$

where  $\phi(t)$  is the angle of rotation of the rotor, and this is allowed to vary. If the rotor spin speed is constant then  $\phi(t) = \Omega t$ , where  $\Omega$  is the spin speed, and  $\dot{\phi} = \Omega$ . Applying the transformation gives, for example

$$\begin{Bmatrix} u \\ v \end{Bmatrix} = \mathbf{T}_2 \begin{Bmatrix} \tilde{u} \\ \tilde{v} \end{Bmatrix}. \quad (14)$$

The displacements in the rotating frame are

$$\begin{Bmatrix} \tilde{u} \\ \tilde{v} \end{Bmatrix} = \mathbf{T}_2^{-1} \begin{Bmatrix} u \\ v \end{Bmatrix} = \mathbf{T}_2^T \begin{Bmatrix} u \\ v \end{Bmatrix}. \quad (15)$$

This transformation must be used for each pair of coordinates, and with the definition of the physical nodal displacements in Eq. (1) this requires an  $8 \times 8$  block diagonal transformation matrix, called  $\mathbf{T}_8(t)$ , with four  $2 \times 2$  blocks given by  $\mathbf{T}_2(t)$ . Similarly transforming the internal variables given in Eq. (2) requires the  $4 \times 4$  block diagonal transformation matrix  $\mathbf{T}_4(t)$  consisting of two blocks given by  $\mathbf{T}_2(t)$ .

We now have to transform the expressions for the elastic force, Eq. (3), using

$$\tilde{\mathbf{q}}_e = \mathbf{T}_8^T \mathbf{q}_e, \quad \mathbf{Q}_e = \mathbf{T}_8 \tilde{\mathbf{Q}}_e, \quad \tilde{\mathbf{p}}_e = \mathbf{T}_4^T \mathbf{p}_e \quad (16)$$

Thus

$$\mathbf{Q}_e = -\mathbf{T}_8 \mathbf{K}_e \mathbf{T}_8^T \mathbf{q}_e + \sum_{i=1}^m \mathbf{T}_8 \mathbf{B}_i \mathbf{T}_4^T \mathbf{p}_{ei} \quad (17)$$

and

$$\mathbf{T}_4 \mathbf{C}_i \mathbf{T}_4^\top \dot{\mathbf{p}}_{ei} + \mathbf{T}_4 \mathbf{C}_i \mathbf{T}_4^\top \mathbf{p}_{ei} + \mathbf{T}_4 \mathbf{H}_i \mathbf{T}_4^\top \mathbf{p}_{ei} = \mathbf{T}_4 \mathbf{F}_i \mathbf{T}_8^\top \mathbf{q}_e \quad \text{for } i = 1, \dots, m. \quad (18)$$

For an axi-symmetric rotor,

$$\mathbf{T}_8 \mathbf{K}_e \mathbf{T}_8^\top = \mathbf{K}_e, \quad \mathbf{T}_4 \mathbf{C}_i \mathbf{T}_4^\top = \mathbf{C}_i, \quad \mathbf{T}_8 \mathbf{B}_i \mathbf{T}_4^\top = \mathbf{B}_i \quad (19)$$

However,

$$\mathbf{T}_4 \mathbf{C}_i \mathbf{T}_4^\top = \dot{\phi} \frac{\ell_e}{6} \begin{bmatrix} 0 & 2 & 0 & 1 \\ -2 & 0 & -1 & 0 \\ 0 & 1 & 0 & 2 \\ -1 & 0 & -2 & 0 \end{bmatrix} \equiv \dot{\phi} \mathbf{D}_i. \quad (20)$$

Hence the force in stationary frame of reference is

$$\mathbf{Q}_e = -\mathbf{K}_e \mathbf{q}_e + \sum_{i=1}^m \mathbf{B}_i \mathbf{p}_{ei} \quad (21)$$

where

$$\mathbf{C}_i \dot{\mathbf{p}}_{ei} + \dot{\phi} \mathbf{D}_i \mathbf{p}_{ei} + \mathbf{H}_i \mathbf{p}_{ei} = \mathbf{F}_i \mathbf{q}_e \quad \text{for } i = 1, \dots, m. \quad (22)$$

Note that the only difference that the rotation makes is to introduce a skew-symmetric term  $\mathbf{D}_i$  into the internal variable equation. Of course there will also be the gyroscopic effects from the inertial terms, and a skew-symmetric contribution to the stiffness matrix if any internal viscous damping is present.

#### 4. The shaftline model of a rotating machine

Those nodes that are associated with a viscoelastic shaft element have four physical degrees of freedom (two translations and two rotations) and  $2m$  internal variables ( $m$  in each plane). The assembly process can proceed by reordering the element degrees of freedom in the above development so that the degrees of freedom for each node are grouped together [15]. This would require the assembly in state space. The alternative, adopted here, is to keep the physical and internal variables separate. This has the advantage that the mass, gyroscopic and stiffness matrices for the physical degrees of freedom in both the rotor and stator may be assembled in the normal way. The equations of motion in terms of the global physical degrees of freedom,  $\mathbf{q}$ , and the global internal variable vectors,  $\mathbf{p}$ , in stationary frame of reference, are

$$\mathbf{M}\ddot{\mathbf{q}} + \dot{\phi} \mathbf{G}\dot{\mathbf{q}} + \mathbf{K}\mathbf{q} = \mathbf{B}\mathbf{p} + \mathbf{f} \quad (23)$$

and

$$\mathbf{C}\dot{\mathbf{p}} + \dot{\phi} \mathbf{D}\mathbf{p} + \mathbf{H}\mathbf{p} = \mathbf{F}\mathbf{q} \quad (24)$$

where the ordering of  $\mathbf{q}$  is based on the usual four degrees of freedom per node, where each node is taken in order.  $\mathbf{M}$  and  $\mathbf{G}$  are the standard mass and gyroscopic matrices with contributions from both the shaft and the disks. The external force,  $\mathbf{f}$ , arises from unbalance and other sources. For simplicity we assume that there are no degrees of freedom in the stator, although including these is straight-forward. Damping in the stator is easily included by adding the standard damping matrix into Eq. (23). The order in the internal variables is taken as  $\mathbf{p} = [\mathbf{p}_{11}^\top \quad \mathbf{p}_{21}^\top \quad \dots \quad \mathbf{p}_{n1}^\top \quad \mathbf{p}_{12}^\top \quad \dots \quad \mathbf{p}_{nm}^\top]^\top$  where  $\mathbf{p}_{ji}$  denotes the internal variable vector of length 2 associated with node  $j$  and eigenvalue  $b_j$  and  $n$  is the number of nodes. The matrices  $\mathbf{C}$ ,  $\mathbf{D}$  and

$\mathbf{H}$  are then block diagonal of the form (only  $\mathbf{C}$  given)

$$\mathbf{C} = \begin{bmatrix} \mathbf{C}_{1(11)} & \mathbf{C}_{1(12)} & & & \\ \mathbf{C}_{1(21)} & \mathbf{C}_{1(22)} + \mathbf{C}_{1(11)} & \mathbf{C}_{1(12)} & & \\ & \mathbf{C}_{1(21)} & \mathbf{C}_{1(22)} + \mathbf{C}_{1(11)} & \mathbf{C}_{1(12)} & \\ & & \ddots & \ddots & \\ & & \mathbf{C}_{m(21)} & \mathbf{C}_{m(22)} + \mathbf{C}_{m(11)} & \mathbf{C}_{m(12)} \\ & & & \mathbf{C}_{m(21)} & \mathbf{C}_{m(22)} \end{bmatrix} \quad (25)$$

where

$$\mathbf{C}_i = \begin{bmatrix} \mathbf{C}_{i(11)} & \mathbf{C}_{i(12)} \\ \mathbf{C}_{i(21)} & \mathbf{C}_{i(22)} \end{bmatrix}. \quad (26)$$

The coupling matrices  $\mathbf{B}$  and  $\mathbf{F}$  have a similar form due to the relationship given in Eq. (7). They also have a similar form to Eq. (25) except that the submatrices have dimension  $4 \times 2$  for  $\mathbf{B}$  and  $\mathbf{F}$ , rather than  $2 \times 2$  for  $\mathbf{C}$ .

The eigenvalues, eigenvectors and forced response are easily computed from the following state space form of Eqs. (23) and (24),

$$\frac{d}{dt} \begin{Bmatrix} \mathbf{q} \\ \dot{\mathbf{q}} \\ \mathbf{p} \end{Bmatrix} = \begin{bmatrix} \mathbf{0} & \mathbf{I} & \mathbf{0} \\ -\mathbf{M}^{-1}\mathbf{K} & -\dot{\phi}\mathbf{M}^{-1}\mathbf{G} & \mathbf{M}^{-1}\mathbf{B} \\ \mathbf{C}^{-1}\mathbf{F} & \mathbf{0} & -\mathbf{C}^{-1}(\mathbf{H} + \dot{\phi}\mathbf{D}) \end{bmatrix} \begin{Bmatrix} \mathbf{q} \\ \dot{\mathbf{q}} \\ \mathbf{p} \end{Bmatrix} + \begin{Bmatrix} \mathbf{0} \\ \mathbf{M}^{-1}\mathbf{f} \\ \mathbf{0} \end{Bmatrix}. \quad (27)$$

#### 5. Numerical example

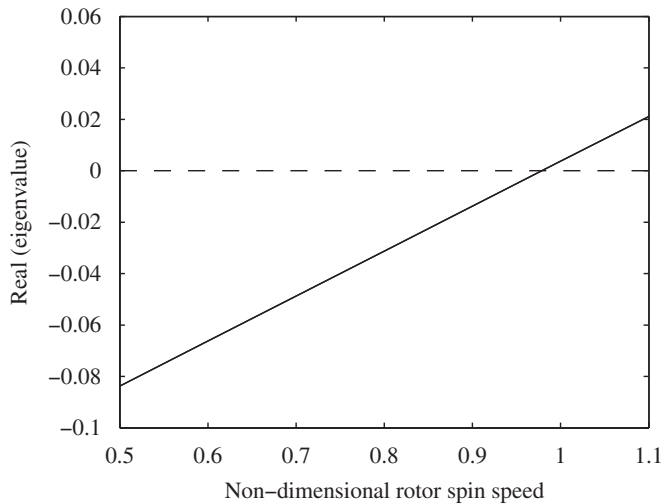
The example from Roy et al. [6] will be used to demonstrate the approach given here. It should be emphasized that the estimated eigenvalues should be identical as the model is the same, but the analysis approach adopted is different. Because of this, only the basic example will be given to verify the approach developed in this paper, as the other results given by Roy et al. [6] may be reproduced easily. The key result is the stability limit speed, that is the maximum rotor spin speed for which the machine is stable.

The machine considered is shown schematically in Fig. 2, and consists of an overhung disk on one end, and a single bearing at the other end. The rotor has a length of 0.75 m and a diameter of 0.05 m. The disk has thickness 0.03 m and diameter 0.15 m. The bearing is long, in the sense that the shaft is constrained to have zero rotation at the bearing. The shaft is able to deflect transversely at the bearing, and the support has stiffness 500 GN/m and damping 1.5 Ns/m in both transverse directions. The shaft and disk are made of aluminium, of density 2750 kg/m<sup>3</sup> and Young's modulus  $E = 71.3$  GPa. The frequency dependent properties of the material are given by the ADF model with a single internal variable ( $m = 1$ ), with  $b_1 = 8000$ ,  $\alpha_1 = 8000$  and  $\delta_1 = 4.7766 \times 10^6$ .

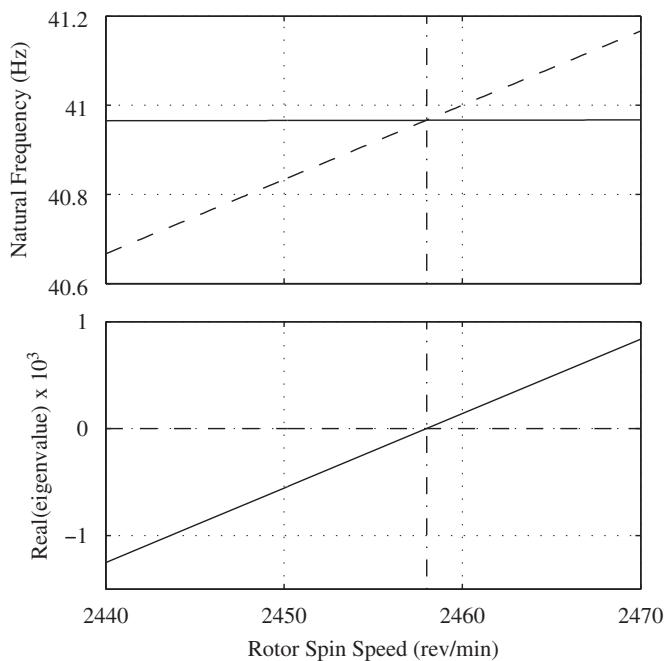
The first forward whirling mode is the first to go unstable and Fig. 3 shows the real part of the corresponding eigenvalue as a function of rotor spin speed. The spin speed is non-dimensionalized with the estimate of the first natural frequency



Fig. 2. A schematic of the example machine.



**Fig. 3.** The variation of the real part of the first forward whirling eigenvalue with the non-dimensional rotor spin speed.



**Fig. 4.** The variation of the first forward whirling natural frequency and the real part of the corresponding eigenvalue with the rotor spin speed. The dashed lines are the 1X line in the upper plot and the stability boundary in the lower plot. The dot-dashed lines are at 2458 rev/min.

given by Roy et al. [6], so that the plot is identical to that given by Roy et al. Fig. 4 shows a zoomed plot of both the first forward whirling natural frequency as a function of rotor spin speed and also the real part of the corresponding eigenvalue. This highlights that the stability limit speed is at the first forward whirling critical speed of 2458 rev/min. Note that the line in Fig. 3 is not zero at a non-dimensional rotor spin speed of 1 because the speed is non-dimensionalized with respect to an estimate of the first natural frequency, not the actual critical speed.

## 6. Conclusions

This paper has developed a novel approach to the analysis of rotating machines where the shaft is made of viscoelastic material

that has frequency dependent properties. The material is modelled using the internal variable method, where extra degrees of freedom are introduced into the equations of motion to model the frequency dependence of the material using a state space form with constant matrices. The difficulty in rotating machines, where the damping is in the rotating part of the system, is that the velocity in the rotating frame must be transformed into the stationary frame. With constant viscous damping in the shaft this leads to skew-symmetric terms in the stiffness matrix that are destabilizing. The new feature of the proposed method is that internal variables used to model the frequency dependent material properties are also transformed into the stationary frame of reference and this leads to skew-symmetric terms in the equations for the internal variables. The proposed approach is easily implemented in shaft-line models of rotating machines, as the internal variables merely add an extra forcing term into the standard equations of motion. Of course the differential equations relating to the internal variables must also be solved simultaneously. The method was verified using an example from the literature.

## Acknowledgement

The authors acknowledge the support of the Royal Society through an India-UK Science Network.

## References

- [1] Bhattacharyya K, Dutt JK. Unbalance response and stability analysis of horizontal rotor systems mounted on nonlinear rolling element bearings with viscoelastic supports. *Journal of Vibration and Acoustics* 1997;119(4): 539–44, doi:10.1115/1.2889757.
- [2] Panda KC, Dutt JK. Design of optimum support parameters for minimum rotor response and maximum stability limit. *Journal of Sound and Vibration* 1999;223(1):1–21, doi:10.1006/jsvi.1998.2062.
- [3] Dutt JK, Toi T. Rotor vibration reduction with polymeric sectors. *Journal of Sound and Vibration* 2003;262(4):769–93, doi:10.1016/S0022-460X(02)01081-7.
- [4] Bormann A, Gasch R. Damping and stiffness coefficients of elastomer rings and their application in rotor dynamics: Theoretical investigations and experimental validation. In: Sixth IFTOMM international conference on rotor dynamics, Sydney, Australia; 2002. p. 628–44.
- [5] Friswell MI, Sawicki JT, Inman DJ, Lees AW. The response of rotating machines on viscoelastic supports. *International Review of Mechanical Engineering* 2007;1(1):32–40.
- [6] Roy H, Dutt JK, Datta PK. Dynamics of a viscoelastic rotor shaft using augmenting thermodynamic fields—a finite element approach. *International Journal of Mechanical Sciences* 2008;50(4):845–53, doi:10.1016/j.ijmecsci.2007.08.007.
- [7] Genta G. Time-domain simulation of rotors with time-domain simulation of rotors with hysteretic damping. In: Ninth international conference on vibrations in rotating machinery, IMechE, Exeter, UK; 2008. p. 799–810.
- [8] Adhikari S. Eigenrelations for nonviscously damped system. *American Institute of Aeronautics and Astronautics Journal* 2001;39(8):1624–30, doi:10.2514/2.1490.
- [9] Adhikari S, Woodhouse J. Identification of damping part 2: non-viscous damping. *Journal of Sound and Vibration* 2001;243(1):63–88, doi:10.1006/jsvi.2000.3392.
- [10] Woodhouse J. Linear damping models for structural vibration. *Journal of Sound and Vibration* 1998;215(3):547–69, doi:10.1006/jsvi.1998.1709.
- [11] Bagley RL, Torvik PJ. Fractional calculus—a different approach to the analysis of viscoelastically damped structures. *American Institute of Aeronautics and Astronautics Journal* 1983;21(5):741–8.
- [12] Bagley RL, Torvik PJ. Fractional calculus in the transient analysis of viscoelastically damped structures. *American Institute of Aeronautics and Astronautics Journal* 1985;23(6):918–25.
- [13] Golla DF, Hughes P. Dynamics of viscoelastic structures—a time domain, finite element formulation. *Journal of Applied Mechanics* 1985;52(4):897–906.
- [14] McTavish DJ, Hughes PC. Modeling of linear viscoelastic space structures. *Journal of Vibration and Acoustics* 1993;115(1):103–13, doi:10.1115/1.2930302.
- [15] Lesiutre GA, Mingori DL. Finite-element modeling of frequency-dependent material damping using augmenting thermodynamic fields. *Journal of Guidance, Control and Dynamics* 1990;13(6):1040–50.
- [16] Lesiutre GA. Finite elements for dynamic modeling of uniaxial rods with frequency dependent material properties. *International Journal of Solids and Structures* 1992;29(12):1567–79, doi:10.1016/0020-7683(92)90134-F.

- [17] Lesieutre GA, Bianchini E. Time domain modeling of linear viscoelasticity using anelastic displacement fields. *Journal of Vibration and Acoustics* 1995;117(4):424–30, doi:[10.1115/1.2874474](https://doi.org/10.1115/1.2874474).
- [18] Lesieutre GA, Lee U. A finite element for beams having segmented active constrained layers with frequency-dependent viscoelastics. *Smart Materials and Structures* 1996;5(5):615–27, doi:[10.1088/0964-1726/5/5/010](https://doi.org/10.1088/0964-1726/5/5/010).
- [19] Rogers LC, Johnson CD, Keinholt DA. The modal strain energy finite element method and its application to damped laminated beams. *The Shock and Vibration Bulletin* 1981; 51.
- [20] Inman DJ. Vibration analysis of viscoelastic beams by separation of variables and modal analysis. *Mechanics Research Communications* 1989;16(4): 213–8, doi:[10.1016/0093-6413\(89\)90025-6](https://doi.org/10.1016/0093-6413(89)90025-6).
- [21] Banks HT, Inman DJ. On damping mechanisms in beams. *Journal of Applied Mechanics* 1991;58(3):716–23, doi:[10.1115/1.2897253](https://doi.org/10.1115/1.2897253).
- [22] Friswell MI, Inman DJ, Lam MJ. On the realisation of GHM models in viscoelasticity. *Journal of Intelligent Material Systems and Structures* 1997;8(11):986–93, doi:[10.1177/1045389X9700801106](https://doi.org/10.1177/1045389X9700801106).
- [23] Lesieutre GA, Govindswamy K. Finite element modeling of frequency-dependent and temperature-dependent dynamic behavior of viscoelastic materials in simple shear. *International Journal of Solids and Structures* 1996;33(3):419–32, doi:[10.1016/0020-7683\(95\)00048-F](https://doi.org/10.1016/0020-7683(95)00048-F).
- [24] Brackbill CR, Lesieutre GA, Smith EC, Govindswamy K. Thermomechanical modelling of elastomeric materials. *Smart Materials and Structures* 1996;5(5):529–39, doi:[10.1088/0964-1726/5/5/003](https://doi.org/10.1088/0964-1726/5/5/003).
- [25] Silva LA, Austin EM, Inman DJ. Time-varying controller for temperature-dependent viscoelasticity. *Journal of Vibration and Acoustics* 2005;127(3): 215–22, doi:[10.1115/1.1897740](https://doi.org/10.1115/1.1897740).
- [26] Friswell MI, Penny JET, Garvey SD, Lees AW. *Dynamics of rotating machines*. Cambridge University Press; 2010.